Paper No.
7408

NACE INTERNATIONAL CORROSION 2016 CONFERENCE & EXPO

Hydrodynamic and Phase Wetting Criteria to Assess Corrosion Risk in Two-Phase Oil-Water Pipe Flow

Luciano D. Paolinelli
Institute for Corrosion and Multiphase Technology, Ohio University
342 W. State Street
Athens, OH 45701
USA

Srdjan Nesic
Institute for Corrosion and Multiphase Technology, Ohio University
342 W. State Street
Athens, OH 45701
USA

ABSTRACT

Two-phase oil-water flow is commonly found in the oil industry. The occurrence of water can lead to internal corrosion of the metallic pipes besides other possible degradation phenomena such as environmentally assisted cracking. When water phase is fully entrained into the oil phase, internal corrosion of carbon steel is not likely to occur. Full entrainment of water into oil depends on operating flow conditions, physicochemical properties of both fluids and phase wetting characteristics for the pipe material used. This paper presents a set of hydrodynamic and phase wetting criteria to assess if free water will be in contact with internal pipe walls; and thus, to primarily determine corrosion risk. Experimental data of oil-water pipe flows is shown and compared with theoretical calculations.

Key words: oil-water flow; entrainment; phase wetting; corrosion

INTRODUCTION

In the oil industry, water can be co-produced with oil. Two-phase oil-water flow is commonly encountered in well tubing, and production and transportation pipelines. The produced saline water can be extremely corrosive to carbon steel due to dissolved gases such as CO_2 and H_2S.[1, 2] When this water is in contact with the metallic pipe wall (scenario called water wetting), this can lead to internal corrosion as well as other possible degradation phenomena such as environmentally assisted cracking. The presence of the hydrocarbon phase can drastically reduce corrosion rates due to one or a combination of phenomena that can be roughly summarized as:

a) Entrainment of the produced water phase into the flowing oil phase: Since produced oils are generally less dense than produced water, the water tends to occupy the pipe bottom or low

points of pipeline sections (e.g. dead legs, inflections due to terrain variations), leading to water wetting. Thus, if produced water is fully dispersed in oil (oil as continuous phase), water wetting is mostly avoided and corrosion occurrence is reduced almost to zero.[3] Full dispersion or entrainment of water into oil is only possible if the turbulent velocity fluctuations in the oil flow are sufficient to disrupt the water phase into droplets and keep them suspended against gravity, preventing them from contacting the pipe wall. In the case when turbulent force is not enough to effectively suspend water droplets, it will depend on other factors such as pipe wall wettability (hydrophilic or hydrophobic nature of the surface) whether settled droplets are re-entrained by the oil flow or remain adhered to the pipe wall. In the latter case, droplets congregate at the bottom of the pipe forming separated water streams, leading to water wetting.

b) Inhibitive effects related to adsorbed or precipitated organic compounds from crude oil and produced water: It has been reported that crude oil natural organic compounds can reduce corrosion rate since they adsorb onto the pipe surface forming protective films that isolate the surface from aggressive species in the water phase and/or interfere with corrosion processes and even modify corrosion product layers.[4-8] The adsorption of organic compounds can either be direct from the oil phase or from the water phase since polar organics can partition into it. The latter explains why the steel corrosion rate can be greatly reduced in some cases when water cuts (water volume fraction in the total oil-water volume) are very high (e.g. 99 %) and steel surfaces are only exposed to water phase.[5, 8] The organic compounds adsorbed onto the steel surface can also alter its wettability (from hydrophilic to hydrophobic) as discussed elsewhere.[4, 8, 9] This surface change can provide corrosion protection by stabilizing hydrocarbon films even in conditions in which water is the continuous phase.

The present work will only focus on the estimation of how water will be transported in two-phase oil-water pipe flow (entrained or separated, as described under a)). This is the first step of corrosion risk assessment that should be performed independently of the inhibitive nature of the produced hydrocarbons. Then, if operational conditions (e.g. oil velocity, water cut, temperature among others) promote water separation, the possible inhibitive effect of specific crude oil organic compounds (as described under b) could reduce the overall corrosion rates. Moreover, the effect of a solid third phase on water wetting is not treated here. However, it is known that small debris coming from the reservoir can settle at the pipe bottom and hold water increasing the chances of corrosion.[10]

1. Hydrodynamic and Phase Wetting Criteria to Assess Full Water Entrainment in Oil-Water Pipe Flow

1.1. Removal of Settled Water from Low Points by the Oil Flow

The removal of settled or trapped water at low points of the pipeline by the oil flow has been studied by several authors.[11-13] There is a minimum critical oil velocity needed to sweep a certain mass of water (or water batch) resting at a low point of a pipeline (e.g., before an upward bend). Some models have been developed based on the instability of the water layer or the oil-water interface,[11, 13] or the formation of a water plug that is pushed by the oil flow.[13] In this cases, the oil flow is not necessarily assumed as turbulent, and Reynolds numbers (Re) can be quite lower than 2100 at the observed critical oil velocities as discussed by Xu et al..[13] Wicks and Fraser,[12] adapted correlations derived from experiments of axial transport of solid particles to this problem and assumed that all the water is broken up into droplets calculated as in turbulent flow as by Hinze.[14] Pots and Hollenberg,[10] reported that the critical oil velocity can be correlated with the densimetric Froude number as found by Snuverink ook Lansink and Duijvestijn:

$$Fr = \sqrt{\frac{\rho_o}{(\rho_w - \rho_o) g D}} U_m \quad (1)$$

where g is the gravitational acceleration (m/s^2), D is de pipe diameter (m), U_m is the mixture flow velocity (m/s), and ρ_o and ρ_w are the density of the oil and the water (kg/m^3), respectively. The critical Froude number for pipe inclinations larger than 5 degrees was found to be 0.67 in turbulent flow conditions (Re > 2100). Smaller values of Fr apply to lower pipe inclinations.

As mentioned previously, the models above estimate the critical oil velocity needed to sweep existing water settled at a low point. This approach is only useful in cases when water settles due to operational upsets (e.g., shutdowns) and gathers at the low points of the flow lines. In that case, when water-free oil moves at velocity larger than the critical one, it will sweep the settled water downstream the flow line, reducing the corrosion risk.

As shown by Pots and Hollenberg,[10] the 'sweeping' criterion greatly underestimates critical flow velocities to avoid the settling of free water layers in field cases and flow loop laboratory tests where constant water flow rates were maintained. This is not surprising, since the physics related to sweeping an settled water layer by oil flow does not necessarily involve full breakup of the water mass into droplets, and their suspension and coalescence.

1.2. Maximum Water Content that Can Be Entrained in an Oil-Water Flow

1.2.1. Phase Inversion Point

Even if the kinetic energy of the oil-water mixture flow is high enough to maintain full entrainment of the water phase into the oil phase, there exists a critical water content in which the oil can no longer exist as the continuous phase and the water-in-oil dispersion spontaneously turns into an oil-in-water dispersion. This critical water content is called phase inversion point (IP). This is a complex phenomenon that depends on several factors such as physicochemical fluid properties among others.[15, 16] If a pipeline operates with water cut values similar to or larger than IP, it is likely to find the water as a continuous phase and this will lead to water wetting conditions at the pipe wall surface.

1.2.2. Critical Water Concentration at the Pipe Bottom

Phase inversion can also happen in flows with water cuts considerably lower than IP. In general, fully dispersed water-in-oil flows can generate a water concentration gradient due to gravity action (e.g. larger concentration at the pipe bottom). When the water concentration at the pipe bottom exceeds a given critical value ($C_{b,crit}$), generalized coalescence of water droplets occurs, developing water layers and producing water wetting. This critical value should be estimated equal or smaller than the phase inversion point ($C_{b,crit} \leq IP$), as discussed elsewhere.[17] In view of this, it is important to know the value of IP for the specific oil-water system under study. Models for predicting IP are mostly dependent on physical properties of fluids (e.g., oil and water viscosities), and based on correlation of experimental data,[15] or mechanistic models.[16] Unfortunately, due to the complexity of this phenomenon, the available models can fail drastically when predicting IP (up to factor of 2 compared to the measured value). Hence, experimental determination of IP is strongly recommended. It is worth mentioning that there exists a standard which includes the measurement of IP in crude oil-water mixtures.[18] From the arguments above, it is clear that the estimation of the water concentration at the pipe bottom is very important when assessing oil-water flows, and is the focus of the following section.

1.2.3. Estimation of the Dispersed Water Concentration at the Pipe Bottom

Water concentration of dispersed transported water can be successfully estimated by the balance between the flux of water droplets settling by the gravity action and the flux of water droplets dispersed by turbulent hydrodynamic forces. Here, the effect of other hydrodynamic forces such as Saffman type can be neglected.[19] Assuming: that water volume concentration only varies with the vertical coordinate $C(y)$, that the total water mass remains constant throughout the whole pipe section ($\int_A C(y)dA = \varepsilon_w A$), that droplets do not adhere to the pipe surface and that droplet size distribution does not vary with time, the mentioned flux balance can be written as the advection-diffusion-like equation for the vertical direction as presented by Karabelas,[20] and Segev:[19]

$$U_s C - \varepsilon \frac{\partial C}{\partial y} = 0 \tag{2}$$

where U_s is the settling velocity of the water droplets (m/s), ε is the droplet turbulent diffusivity (m^2/s) which can be calculated as:

$$\varepsilon = \zeta \frac{D}{2} \sqrt{\frac{\rho_m f}{2\rho_o}} U_m \tag{3}$$

where f is the Fanning friction factor (calculated for hydraulically smooth pipes,[21] or for hydraulically rough pipe[22]) , ρ_m is the mixture density (kg/m^3) calculated as: $\rho_w \varepsilon_w + \rho_o(1-\varepsilon_w)$, with ε_w as the water holdup (in dispersed flow can be considered as equal to the water cut), and ζ is the dimensionless eddy diffusivity that can be considered as constant ($\zeta \simeq 0.25$) according to Karabelas.[20] However, closer analysis of Karabelas' experimental data indicates that the value of ζ tends to decrease with decreasing Reynolds number (for example: $\zeta \simeq 0.2$ at $Re \simeq 3000$).
The settling velocity of the water droplets can be estimated as:

$$U_s = \sqrt{\frac{4}{3} \frac{d(\rho_w - \rho_o)g}{\rho_o C_D}} \tag{4}$$

where d is the droplet diameter (m), and C_D is the droplet drag coefficient which can be estimated for a large range of droplet Reynolds numbers ($Re_p < 800$) using Schiller-Naumann correlation (solid spheres[23]):

$$C_D = \frac{24}{Re_p}\left(1 + 0.15 {Re_p}^{0.687}\right) \tag{5}$$

The droplet Reynolds number is calculated as:

$$Re_p = \frac{\rho_o d\, U_s}{\mu_o} \tag{6}$$

where μ_o is the dynamic viscosity of the oil (Pa.s). It is worth mentioning that water droplets moving in oil can experience internal recirculation currents which can greatly reduce drag force, making them settle at higher speeds.[24, 25] In this case, the water droplet-oil interface has to be mostly clean or free of surface active compounds which can hamper or impede its motion by partial or total coverage. In general, crude oils contain many organic compounds that can alter the interfaces of the water droplets making them appear as solid-like in the oil flow, so equation (5) is a good approximation. On the other hand, condensate hydrocarbons can have less or no surface active compounds. In general, mineral processed oils, which are usually used in flow loop or other laboratory experiments, do not contain significant amounts of surface active compounds. Thus, in these cases, internal recirculation is likely to

occur. Here, drag coefficient correlations are function of Re_{p} as well as the ratio between water and oil dynamic viscosities ($\lambda = \mu_{\mathrm{w}}/\mu_{\mathrm{o}}$) as Rivkind and Ryskin.[25]

Estimation of dispersed water droplet sizes is crucial to complete the calculation of water concentration. Hinze's model can be used to calculate the size of the maximum stable water droplet (m) for dispersions with water holdups smaller than 5 %:[14]

$$d_{\max} = 0.725 \left(\frac{\sigma}{\rho_{\mathrm{o}}}\right)^{3/5} \epsilon^{-2/5} \tag{7}$$

where ϵ is the mean energy dissipation rate per unit of mass of the oil phase (Watt/kg), and σ is the interfacial oil-water tension (N/m). For dispersions with water holdups equal or larger than 5 %, $d_{\max}$ values become larger than predicted by equation (7) due to the decrease of the disruptive energy in the oil phase when dispersed water volume fraction (ε_{w}) increases. Here, Brauner's model can be used:[21]

$$d_{\max} = \left(6C_{\mathrm{H}} \frac{\varepsilon_{\mathrm{w}}}{(1-\varepsilon_{\mathrm{w}})}\right)^{3/5} \left(\frac{\sigma}{\rho_{\mathrm{o}}}\right)^{3/5} \epsilon^{-2/5} \tag{8}$$

where C_{H} is a constant on the order of 1. Good agreement of predicted $d_{\max}$ values with numerous flow loop experimental data was found when using $C_{\mathrm{H}} \simeq 1.8$.[26] It must be considered that droplet size predictions using equations (7) and (8) are valid for a limited length scale range.[21]

The mean energy dissipation rate per unit of mass of the oil phase is estimated as follows:

$$\epsilon \cong 2 \frac{\rho_{\mathrm{m}} f {U_{\mathrm{o}}}^3}{D\rho_{\mathrm{o}}(1-\varepsilon_{\mathrm{w}})} \tag{9}$$

where U_{o} is the oil phase velocity (m/s), which equals the mixture velocity in dispersed flow if the slip between the oil and the water droplets is neglected ($U_{\mathrm{o}} \simeq U_{\mathrm{m}}$).

Once $d_{\max}$ is known, water droplet size distribution can be estimated using a Rosin-Rammler type equation:[27]

$$V = \exp\left[-11.51 \left(\frac{d}{d_{\max}}\right)^{\delta}\right] \tag{10}$$

where V is the cumulative volume fraction of droplets with diameters larger than d. In this case, equation (10) was arranged as a function of the maximum droplet size. According to the available experimental data, the exponent δ usually ranges between 2 and 3.[27-29] For practical purposes, $\delta = 2.5$ can be used for horizontal flow.

Once droplet size distribution is known, water concentration at the pipe bottom can be calculated by solving numerically equation (2) or using the approximated closed-form solutions offered by Karabelas;[20] for example, using a single droplet size:

$$C_{\mathrm{b}} = \left[1 + 2 \frac{(1-\varepsilon_{\mathrm{w}})}{\varepsilon_{\mathrm{w}}} \frac{I_1(K)}{K} \exp(-K)\right]^{-1} \tag{11}$$

where:

$$K = \frac{DU_{\mathrm{s}}}{2\varepsilon} \tag{12}$$

and $I_1(K)$ is the modified Bessel function of order 1.[20] Equating expression 11 with the critical maximum water concentration value (e.g. $C_{\mathrm{b,crit}} = IP$, as discussed in previous section), the critical oil or mixture velocity value is determined ($U_{\mathrm{o,Ccrit}}$ or $U_{\mathrm{m,Ccrit}}$, respectively). This criterion represents the lowest velocity bound in which water wetting can be avoided by the oil flow.

Mean water droplet size (d_{50} or Sauter mean diameter, d_{32}) can be used to represent whole droplet population and simplify water concentration computation. However, in general, results are more accurate using multiple droplet sizes as discussed by Segev[19] Pots and Hollenberg reported a simpler but less accurate expression for the calculation of water concentration at the pipe bottom.[10]

The model described above is valid only if water droplets do not adhere to the pipe surface (e.g., no water mass is collected at the bottom of the pipe). Therefore, to know whether it can be applied or not, it is important to know if dispersed water drops will sink and adhere at the pipe bottom, as discussed in the next section.

Figure 1 compares predictions of water concentration profiles generated using the present model with experimental data reported elsewhere from crude oil-water horizontal fully dispersed flows in 1 meter-diameter lines.[19] The Rosin-Rammler water droplet distribution (with $\delta = 2.5$) and the Schiller-Naumann drag were used in these calculations. Estimated concentrations show good agreement with experimental data, especially at the pipe bottom, which is the most important location for water wetting assessment.

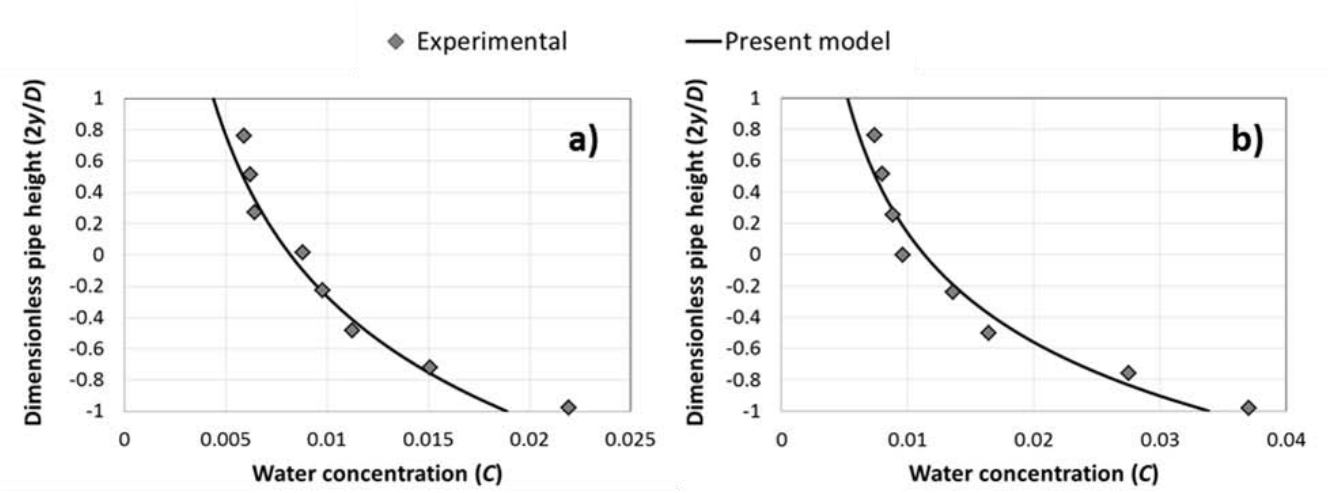

Figure 1: Predicted versus experimental water concentration profiles for crude oil-water flows in 1 meter-diameter lines. a) $\rho_{\mathrm{o}} = 851$ kg/m^3, $\mu_{\mathrm{o}} = 0.0117$ Pa.s, $U_{\mathrm{m}} = 2.02$ m/s, $\varepsilon_{\mathrm{w}} = 0.009$. b) $\rho_{\mathrm{o}} = 853$ kg/m^3, $\mu_{\mathrm{o}} = 0.012$ Pa.s, $U_{\mathrm{m}} = 1.8\ \mathrm{m/s}$, $\varepsilon_{\mathrm{w}} = 0.013$. For both cases, the following parameters were estimated as: $\sigma = 0.025$ N/m, and $\rho_{\mathrm{w}} = 1000$ kg/m^3.

1.3. Calculation of Hydrodynamic Forces to Suspend Water Droplets

1.3.1. Turbulent Forces

Turbulent dispersive forces tend to act against the droplet concentration gradient (as described in equation 2). Therefore, radial turbulent velocity fluctuations in the oil are expected to act mostly accelerating water droplets flowing near the pipe wall towards the pipe core. Bagnold [30] first modeled this concept in problems of suspension and transport of solids in horizontal conduits, equating the gravity force on the particles (F_{g}, N) to the drag force (F_{t}, N) produced by the root mean square (rms) value of the vertical turbulent velocity fluctuations in the continuous phase flow (v', m/s). In this terms,

fulfilling the condition: $F_g \leq F_t$ would be enough to suspend the transported particles (in this case water droplets). Here, droplet gravity force can be expressed as:

$$F_g = \frac{\pi d^3}{6}(\rho_w - \rho_o) g \cos\beta \quad (13)$$

where β is the inclination angle of the conduit or pipe measured from the horizontal (radians). The turbulent suspension force is:

$$F_t = \frac{1}{2}\rho_o \frac{\pi d^2}{4} C_D v'^2 \quad (14)$$

where C_D is the drag coefficient of the water droplet as in equation (5) but evaluated using $Re_p = \rho_o d\, v'/\mu_o$. Equating expressions 13 and 14, a critical droplet size (m) can be obtained:

$$d_{crit} = \frac{3}{4}\frac{\rho_o}{(\rho_w - \rho_o) g \cos\beta} C_D v'^2 \quad (15)$$

Some researchers have simplified $C_D = 1$ and approximated the mean radial turbulent fluctuations (rms) in a pipe as: [21, 31]

$$v' \simeq \sqrt{\frac{\rho_m f}{2\rho_o}} U_m \quad (16)$$

The value of v' also depends on the Reynolds number and decays almost linearly from the magnitude in (16) at the beginning of the logarithmic region in the hydrodynamic boundary layer ($y^+ = 30$) to zero at the wall. [32]

Equation (15) can over-predict d_{crit} for water concentrations larger than ~ 2 % since droplet-continuous phase and interdroplet interactions are neglected. In this case, at least two phenomena affect the force balance on the droplet. First, the effective v'value can decline with droplet concentration.[33] Second, the hydrodynamic interdroplet forces (e.g. lubrication forces[34]) can hamper in this case the effectiveness of the turbulent suspension force on the droplet. These effects are function of the water concentration near the pipe wall. However, they will not be treated here for the sake of discussing other more important concepts.

From equation (15), it is clear that the critical droplet size (d_{crit}) must be compared to the maximum stable droplet size in dispersion (calculated as equation 7 or 8) in the following way to assess full turbulent suspension of all the water mass:

$$d_{crit} \geq d_{max} \quad (17)$$

Then, the critical oil or mixture velocity value is determined ($U_{o,Tcrit}$ or $U_{m,Tcrit}$, respectively) from solving equation (17) ($d_{crit} = d_{max}$).

1.3.2. Boundary Layer Flow Forces and Pipe Surface Wettability

In the case that the oil velocity is not high enough to suspend larger water droplets by the near-wall turbulent forces ($d_{crit} < d_{max}$), these droplets will eventually contact the pipe wall. Contacting droplets can behave quite differently depending on the wettability of the pipe surface; precisely, water-in-oil wetting characteristics.

If pipe surface is hydrophilic (contact angle measured from the inside of the droplet, $\theta < 90°$), the contacting water droplets will adhere and spread in such a way that they can no longer be re-entrained

by the oil flow leading to water rivulets, which will produce a water wetting condition. This statement is based on studies on droplet detachment by external flow action, which indicate that contact angle values of 90° or lower do not allow complete droplet removal from surfaces[35-39]

On the other hand, a hydrophobic surface ($\theta > 90°$) leads to poor or even no attachment of water droplets and allows their re-entrainment by the oil flow, avoiding water wetting. Complete droplet removal from high-contact-angle surfaces in flow conduits has been reported elsewhere.[39-42]

Based on the concepts describe above, for a given hydrophobic pipe surface, there exist a critical oil velocity lower than the calculated using $d_{\mathrm{crit}} = d_{\mathrm{max}}$ (expression 17) but high enough to remove sinking unstable water droplets from surface, producing their re-entrainment and keeping the surface mostly oil-wet. This problem can be modeled analyzing the dynamic stability of water droplets that eventually contact a previously oil-wet pipe surface.

Assuming that once a water droplet comes in contact with the oil-wet pipe wall it instantaneously develops a contact patch proportional to the water-in-oil contact angle (θ) of the oil-water-solid surface system (area enclosed by the dashed line in Figure 2 b). At the same time, the boundary layer-oil flow exerts hydrodynamic forces on it. The hydrodynamic forces can be separated into two orthogonal directions: parallel to the pipe surface (drag force), and normal to the pipe surface (lift force, F_{L} in Figure 2 b). Here, only the latter is assumed to re-entrain the droplet instantaneously, which is the most conservative assumption.

When analyzing the forces on an attached droplet in the direction normal to the pipe surface, the lift force (F_{L}, N) opposes the normal adhesion or surface force (F_{s}, N) and the gravity force (F_{g}, equation 13), as in Figure 2 b. A droplet that sinks and adheres to the pipe surface can be removed if:

$$F_{\mathrm{L}} \geq F_{\mathrm{s}} + F_{\mathrm{g}} \tag{18}$$

The normal adhesion force follows from the oil-water surface tension and the static water-in-oil contact angle (θ, radians):

$$F_{\mathrm{s}} = 2\pi c\sigma \sin\theta \tag{19}$$

where c is the radius of the contact patch of the attached droplet (m) as in Figure 2a (truncated sphere geometry of diameter d' and height h):

$$c = \frac{d'}{2}\sin\theta \tag{20}$$

As the present force assessment is only suitable for surfaces with $90° < \theta < 180°$, d' and h can be consider equal to the unattached droplet diameter (d).

The lift force is estimated as:

$$F_{\mathrm{L}} = \frac{1}{2}\rho_{\mathrm{o}}\frac{\pi d^2}{4}C_{\mathrm{L}}{U_{\mathrm{o,d/2}}}^2 \tag{21}$$

where the lift coefficient of the attached droplet is ($0.1 < Re_{\mathrm{p}} \leq 250$ [43]):

$$C_{\mathrm{L}} = 5.811 - 4.339{Re_{\mathrm{p}}}^{0.0429}\tanh\left(0.9395{Re_{\mathrm{p}}}^{0.3531} - 0.2966\right) + 0.0589\tanh\left(-0.1137Re_{\mathrm{p}} + 2.5386\right) \tag{22}$$

using $Re_{\mathrm{p}} = \rho_{\mathrm{o}} d\, U_{\mathrm{o,d/2}}/\mu_{\mathrm{o}}$. The velocity of the boundary layer-oil flow at the mid height of the attached droplet ($\sim d/2$) can be approximated as (for $0.5 < d^{+}/2 < 150$):

$$U_{o,d/2} = \sqrt{\frac{\rho_m f}{2\rho_o}} U_m \left[a_6 \left(\frac{d^+}{2}\right)^6 + a_5 \left(\frac{d^+}{2}\right)^5 \mp a_4 \left(\frac{d^+}{2}\right)^4 + a_3 \left(\frac{d^+}{2}\right)^3 \mp a_2 \left(\frac{d^+}{2}\right)^2 + a_1 \left(\frac{d^+}{2}\right) \right] \quad (23)$$

where $a_1 = 1.21,\ a_2 = -4.1 \times 10^{-2},\ a_3 = 7.1 \times 10^{-4},\ a_4 = -6.6 \times 10^{-6},\ a_5 = 3.1 \times 10^{-8},\ a_6 = -5.7 \times 10^{-11}$, and $d/2$ is expressed as hydrodynamic wall distance:

$$\frac{d^+}{2} = \frac{\rho_o d}{2\mu_o} \sqrt{\frac{\rho_m f}{2\rho_o}} U_m \quad (24)$$

If $d^+/2 < 0.5$ or $d^+/2 > 150$, regular formulation for viscous sublayer or logarithmic region[32, 44] can be used to calculate boundary layer-oil velocity. The empirical lift force equation reported by Mollinger and Nieuwstadt[45] can be used when $0.3 < d^+/2 < 2$, instead of equation (21).

Combining expressions (13) and (18) to (21) a critical diameter for droplet removal can be obtained (d_{lift} , m):

$$d_{lift}{}^2 \ (\rho_w - \rho_o) g \cos\beta/6 - d_{lift}\ \rho_o C_L {U_{o,d/2}}^2/8 + \sigma \sin^2\theta = 0 \quad (25)$$

Here, only the droplets with diameters equal or larger than d_{lift} will be removed by the boundary layer-oil flow. Therefore, to assure fully dispersed flow, the droplet sizes smaller than d_{lift} need to be suspended by the turbulent forces. The above mentioned requirements are simply satisfied by solving equation (25) simultaneously with equation (15) to get:

$$d_{crit} \geq d_{lift} \quad (26)$$

Then, a critical oil or mixture velocity ($U_{o,Lcrit}$ or $U_{m,Lcrit}$, respectively) lower than $U_{o,Tcrit}$ (calculated using $d_{crit} = d_{max}$, expression 17) is obtained for full water entrainment. In the case that d_{lift} is equal to d_{max}, the calculated oil critical velocity $U_{o,Lcrit}$ is equal to $U_{o,Tcrit}$. It is worth mentioning that if the pipe surface is super hydrophobic (e.g. $\theta \simeq 180°$), no adhering of droplets would occur on pipe wall. Hence, evaluation of d_{lift} is not needed and the critical oil velocity is calculated using equation (11) ($C_b = IP$, to obtain $U_{o,Ccrit}$).

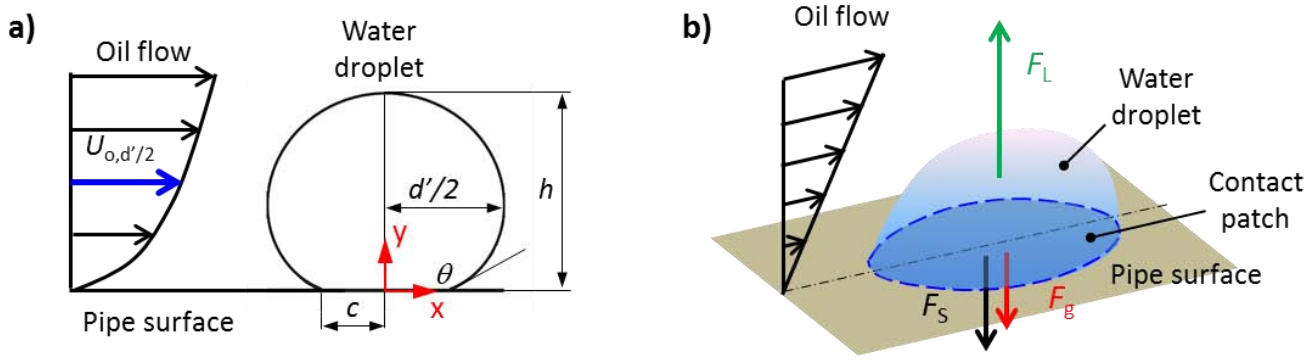

Figure 2: Schematics showing the attachment of the water droplets on the pipe surface under oil flow condition. a) Non-deformed droplet geometry. b) Force diagram on the droplet (normal direction only).

2. Evaluating phase wetting status of internal pipe walls in oil-water flow

From the Introduction, it is clear that full entrainment of water in oil cannot be simply defined by a single criterion (e.g., suspension of droplets by turbulent forces). Therefore, the combination of the criteria described above is needed to account for better and more comprehensive assessment of the transition from oil wet to water wet pipe surfaces. In Figure 3, the flow diagram summarizes the proposed steps to evaluate the phase wetting status of internal pipe walls according to the superficial oil velocity, the transported water cut, the water and oil properties (oil and water densities and viscosities and interfacial oil-water tension), the pipe characteristics (diameter, inclination angle and surface roughness), the oil-water mixture inversion point, and the pipe surface wettability (water-in-oil contact angle).

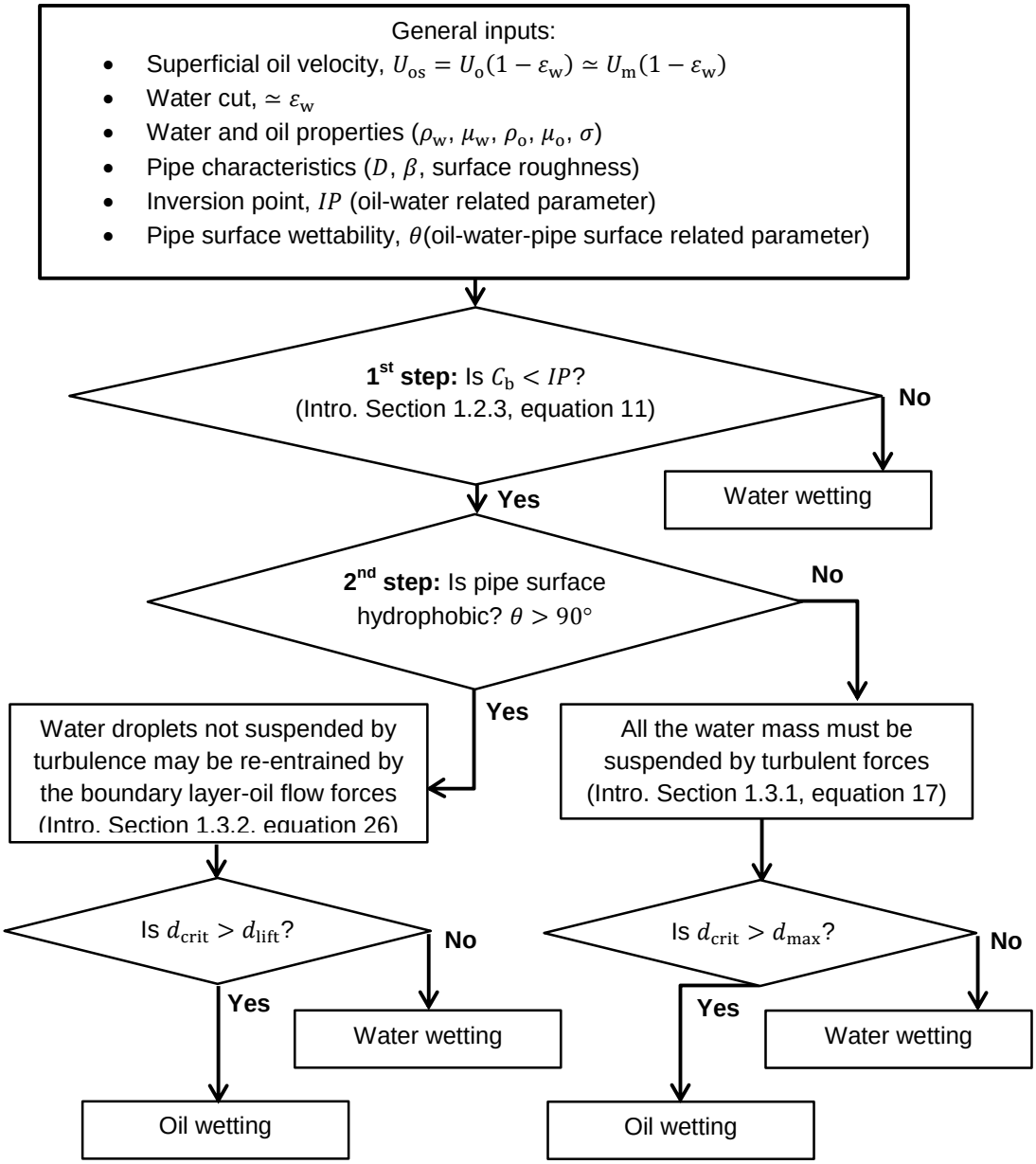

Figure 3: Flow diagram describing the steps and criteria used for assessing phase wetting on internal pipe walls in oil-water flow.

Figure 4 shows examples of calculated phase wetting maps (mixture velocity as a function of water cut) for a light crude oil-water system flowing in horizontal pipe with hydrophilic and hydrophobic internal surfaces. In pipes with hydrophilic surfaces (Figure 4a), the full water-in-oil dispersion boundary is determined by equation (17) ($d_{\mathrm{crit}} = d_{\mathrm{max}}$, dashed black line) at low water cuts. At higher water cuts, equation (17) is satisfied at lower flow velocities than needed to keep the water concentration in oil equal or lower than IP at the pipe bottom ($C_{\mathrm{b}} = IP$, equation 11, dash-dot black line). Hence, the latter concept becomes dominant.

For hydrophobic pipe surfaces (Figure 4b), the full water-in-oil dispersion boundary is pushed to lower flow velocities as per equation (26) ($d_{\mathrm{crit}} = d_{\mathrm{lift}}$, short-dash red line). In this case, pipe surface hydrophobicity allows flow with fully dispersed water phase at half the velocity required for hydrophilic pipe surfaces (Figure 4a). Again, at large water cuts the criterion $C_{\mathrm{b}} \leq IP$ (dash-dot black line) becomes dominant.

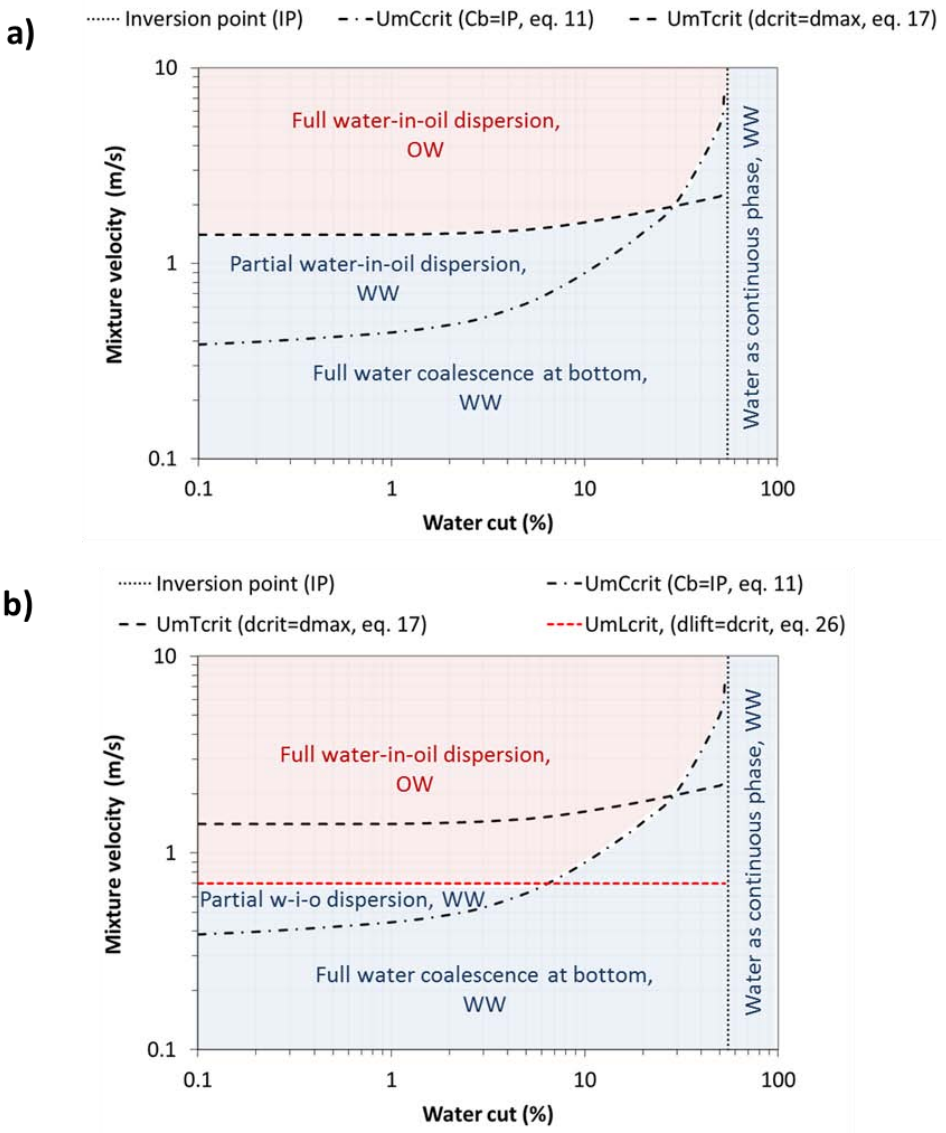

Figure 4: Estimated phase wetting maps (OW: oil wetting, WW: water wetting) in horizontal flow. a) Hydrophilic internal pipe surface ($\theta < 90°$); b) Hydrophobic internal pipe surface, $\theta = 170°$. System properties: $\rho_{\mathrm{o}} = 830$ kg/m^3, $\mu_{\mathrm{o}} = 0.0047$ Pa.s; $\rho_{\mathrm{w}} = 1005$ kg/m^3, $\mu_{\mathrm{w}} = 0.001$ Pa.s, $\sigma = 0.026$ N/m, $IP = 55$ %. Pipe characteristics: $D = 0.1$ m, smooth internal surface.

The equation (26) explains why in some cases dispersions of water in crude oil can be sustained at relatively low flow velocities (less than 1m/s) even without forming stable emulsions.[46]

In view of the present analysis, the characterization of the pipe surface wettability appears to be important to properly assess phase wetting behavior and, consequently, internal corrosion risk. Even though equation (26) is a simplified model, it depends on the quantification of the static water-in-oil contact angle (θ) measured on sessile water drops using representative samples of pipe material and fluids (produced oil and water). This can be achieved by conventional optical methods using a chamber with transparent windows to allow lightning and visualization of the contacting drop as well as the proper conditioning of the fluids (temperature, dissolved gas content, pressure, water pH, etc.) to mimic the real conditions as much as possible. Unfortunately, most of the crude oils are dark, making optical evaluation of the water droplet contact extremely difficult. Recently, Richter et al. have shown that it is possible to qualify the effect of crude oil on the water-in-oil contact angle by observing water droplet contact on crude-oil pre-wetted steel surfaces immersed in clear model oil.[8] Although the method requires future refinement, it is useful to roughly evaluate whether a given dark crude oil under study alters steel surface wettability or not.

In the next sections, available phase wetting experimental data obtained in a large-scale flow loop will be compared against the mechanistic model introduced above.

EXPERIMENTAL PROCEDURE

Oil-water flow experiments were conducted at the Institute for Corrosion and Multiphase Technology (ICMT), Ohio University† in a large-scale inclinable multiphase flow loop with an internal diameter of 0.1 m and fluid separation capabilities. A detailed description of the flow facility and instrumentation is found elsewhere.[46-48] During experiments, phase wetting regime (oil wet or water wet pipe surface) was capture by means of an arrangement of flush mounted conductivity probes (with DC excitation) along a carbon steel test section circumference. All the experiments were performed at room temperature (~25 °C).

Table 1 list the information about the properties (at 25 °C) of the oil and the water used in the experiments and the respective references to authors. All the listed crude oils showed to alter the wettability of carbon steel surfaces as reflected by the extremely high values of the measured water-in-oil contact angles ($\theta = 180°$ [8]). In these cases, the phase wetting boundary calculations will be performed using a contact angle of $175°$. This allows for more conservative results, since water droplets are able to adhere to the pipe surface but have very poor adhesion. On the other hand, carbon steel surfaces wetted by the tested model oil (LVT 200† paraffinic oil) showed typical hydrophilic behavior.[4, 8, 49]

† Trade name

Table 1: List of properties of the oil and water used in the phase wetting experiments.

Flow case	ρ_o (kg/m^3)	ρ_w (kg/m^3)	μ_o (Pa.s)	μ_w (Pa.s)	σ (N/m)	IP (%)	θ (deg)
Model oil and 1% wt. NaCl water	823 (2)	1005	0.0027 (2)	0.001	0.04 (2)	45 (4)	73 (2)
Super light crude oil and 1% wt. NaCl water	778 (1)	1005	0.0016 (1)	0.001	0.025 (1)	45 (4)	180 (3)
Extra light crude oil and 1% wt. NaCl water	830 (1)	1005	0.0047 (1)	0.001	0.026 (1)	55 (4)	180 (3)
Medium crude oil and 1% wt. NaCl water	878 (1)	1005	0.022 (1)	0.001	0.023 (1)	60 (4)	180 (3)

(1) reference [46]
(2) reference [49]
(3) reference [8]
(4) measured in a stirred vessel using a high frequency impedance probe.

RESULTS AND DISCUSSION

Figure 5 shows the measured and predicted phase wetting transition mixture flow velocities versus water cut for model oil (properties listed in Table 1) in horizontal flow. Phase wetting transition mixture velocities measured by Cai et al.[47] and Kee[49] (black crosses and back squares, respectively) are similar for water cuts larger than 1 %. The phase wetting transition estimated as proposed in this work show a good agreement with the available experimental data. As the carbon steel pipe surface is hydrophilic ($\theta < 90°$), it is needed to suspend all the flowing water mass with the action of turbulent flow forces (modeled by equation 17, dashed black line). Unfortunately, there is no experimental data in this case to check phase wetting transition behavior at water cuts larger than 15 %, in which criterion of critical water concentration at the pipe bottom (modeled by equation 11, dash-dot black line) becomes dominant. At low water cuts (≤ 1%), the measured phase wetting transition velocities show to be lower than predicted. This may be due to fact that when free water content is significantly small, the used phase wetting sensors become less sensitive and overlook the existence of, for example, small rivulets of water at the pipe bottom.

For hydrophobic pipe surfaces, different phase wetting transition behavior is seen. For example, the experimental phase wetting transition data for the super light crude oil (black triangles, Figure 6[46]) show lower mixture velocities than predicted by equation (17) (dashed black line) in the tested range of water cuts. According to equation (26) (short-dash red line in Figure 6, $\theta = 175°$), the water droplets that cannot be suspended by the turbulent velocity fluctuations of the oil flow can still be removed once they contact the pipe wall at a mixture flow velocity larger than about 0.6 m/s. However, as explained in Introduction Section 2, if water concentration at the pipe bottom becomes critical ($C_b = IP$) massive coalescence of water droplets can occur leading to water wetting. Hence, depending on the water cut, mixture velocities larger than 0.6 m/s are needed to keep water concentration at the pipe bottom below

the critical value as estimated by equation (11). This bound (dash-dot black line in Figure 6) shows very good agreement with the experimental phase wetting transition data.

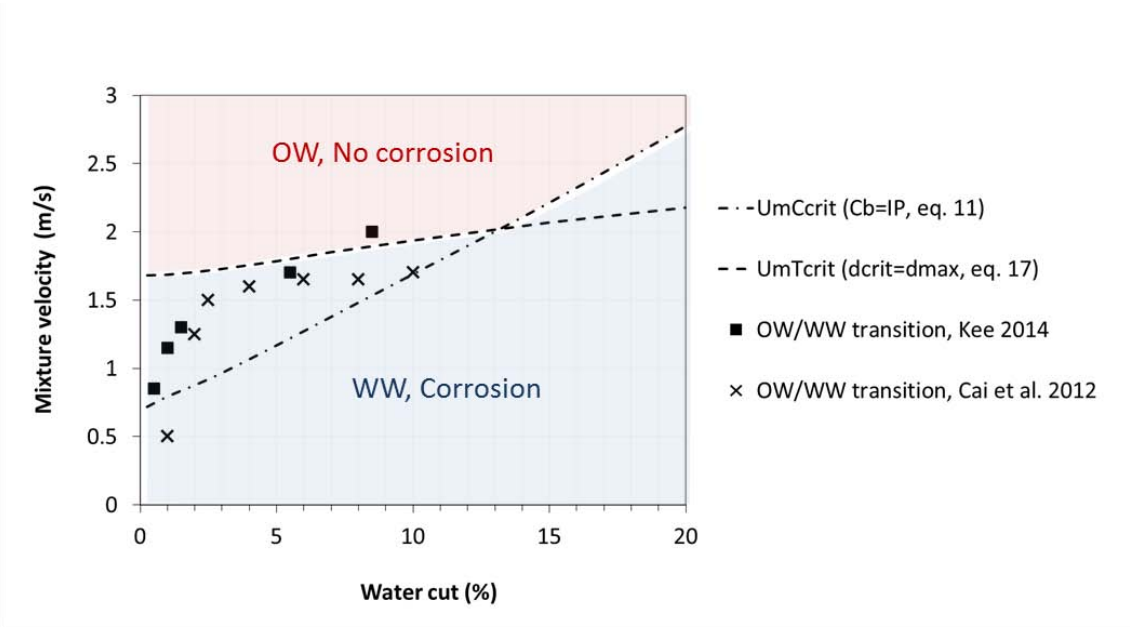

Figure 5: Measured and estimated phase wetting transition (OW: oil wetting, WW: water wetting) for model oil in horizontal flow. Hydrophilic and hydraulically smooth internal pipe surface. Oil properties listed in Table 1.

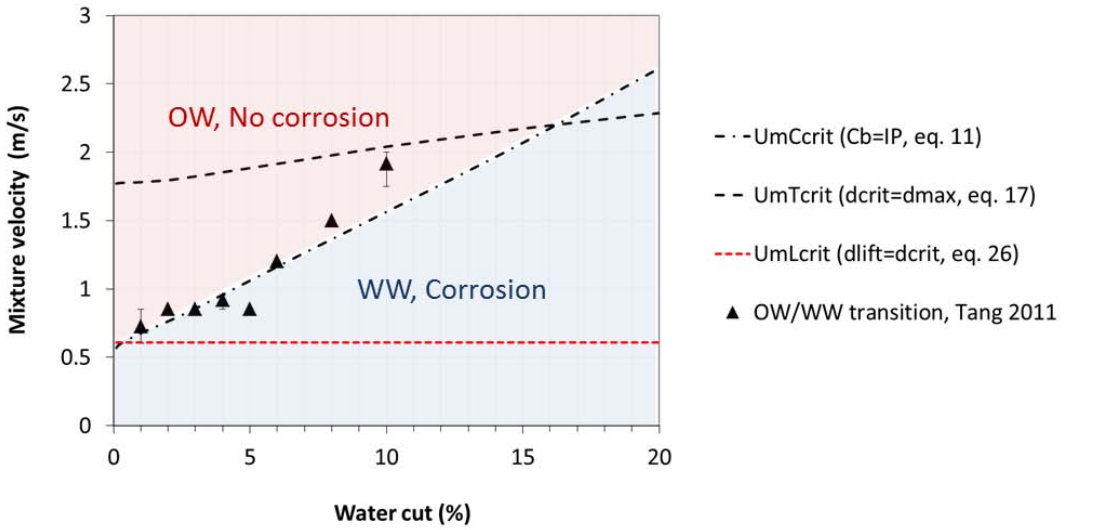

Figure 6: Measured and estimated phase wetting transition (OW: oil wetting, WW: water wetting) for the super light crude oil in horizontal flow. Hydrophobic and hydraulically smooth internal pipe surface. Oil properties listed in Table 1.

The extra light crude oil (Figure 7) also shows the experimental phase wetting transition (black diamonds [46]) at lower mixture velocities than predicted by equation (17) (dashed black line). It can be seen that at water cuts lower than about 6 %, the measured phase wetting transition is at a somewhat constant mixture velocity of about 0.65 m/s. This is in close agreement with the lowest mixture velocity bound of about 0.6 m/s predicted by equation (26) (short-dash red line in Figure 7, $\theta = 175°$). For water cuts larger than 6 %, the measured phase wetting transition is very well described by the critical water concentration bound calculated by equation (11) (dash-dot black line in Figure 7).

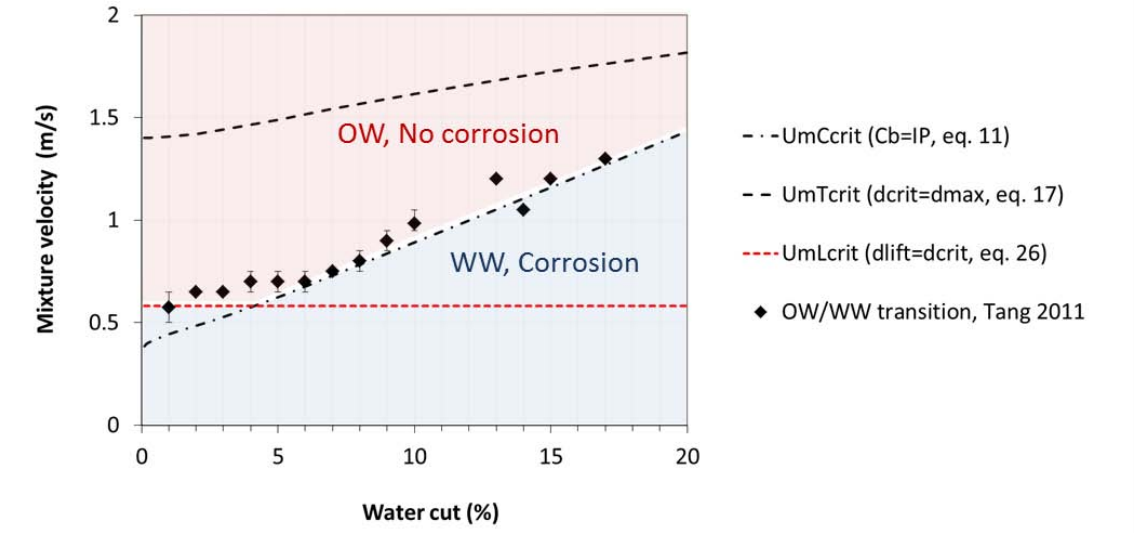

Figure 7: Measured and estimated phase wetting transition (OW: oil wetting, WW: water wetting) for the extra light crude oil in horizontal flow. Hydrophobic and hydraulically smooth internal pipe surface. Oil properties listed in Table 1.

Figure 8 shows the experimental phase wetting transition data obtained for the medium crude oil (black circles[46]). Again, phase wetting transition shows at lower velocities than predicted by equation (17) (dashed black line) as seen in all the cases when in hydrophobic internal surfaces are present (Figures 6 and 7). In this case, mixture flow velocities larger than about 0.5 m/s are needed to remove water droplets that contact the pipe wall (equation 26 using $\theta = 175°$, short-dash red line in Figure 8). The transition from turbulent to laminar flow ($Re = 2100$) is at about 0.55 m/s. Hence, the existence of well disrupted water droplets will only occur at mixture velocities larger than 0.55 m/s, value which now defines the lowest mixture velocity bound for phase wetting transition (dot blue line in Figure 8). This limit agrees well with the measured phase wetting transition at water cuts equal or lower than about 7 %. For water cuts higher than 7 %, the experimental phase wetting transition is close to the bound predicted by equation (11) (dash-dot black line in Figure 8).

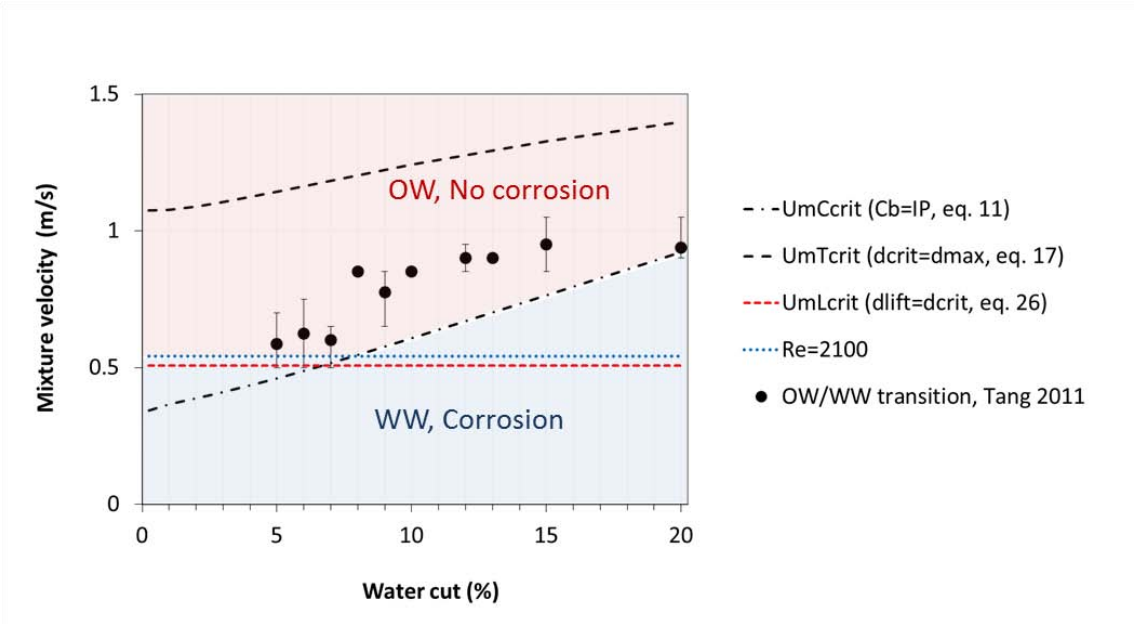

Figure 8: Measured and estimated phase wetting transition (OW: oil wetting, WW: water wetting) for the medium crude oil in horizontal flow. Hydrophobic and hydraulically smooth internal pipe surface. Oil properties listed in Table 1.

It has been shown that accounting for the wettability behavior of the internal pipe surface (via equation 26) is very important in understanding the possible entrainment of the water phase in oil-water pipe flow; and thus, whether corrosion will be likely to occur or not.

In general, the hydrodynamic criteria introduced in this work to predict full water entrainment by oil flow agree well with all the phase wetting transition data (oil wet to water wet) obtained in large scale laboratory flow loop using model oil as well as crude oils. This improved model, based on a simplified approach to the physics of dispersed water droplets and their contact with the pipe wall, incorporates some of the physicochemical influences of the oil-water interface (e.g. inversion point) and the oil-water-solid pipe surface interfaces (e.g. water-in-oil contact angle) that have been overlooked by other multiphase flow models.[21, 31]

It is worth mentioning that all the multiphase flow calculations proposed in Section 1 assume that water droplets will be disrupted only by the intrinsic turbulence of the pipe flow and that stable emulsions are not formed. This leads to a conservative estimation of the critical flow velocities for phase wetting transition. In practice, high flow shear rates introduced by pumps and choke valves can break up the water phase into smaller drop sizes than predicted by equations (7) and (8) using the mean energy dissipation rate in the oil flow (ϵ) as calculated in equation (9). These smaller water droplet sizes can be then entrained at lower flow velocities. If no or partial emulsification occurs, water droplets will then eventually coalesce downstream the flow line until reaching the equilibrium sizes inherent to pipe flow, which can be reasonably predicted as shown in Section 1. In case of emulsification, the coalescence and dropout of water droplets results more unlikely, even in cases where flow velocities are low.

It must be noticed that prediction of the phase wetting transition in three-phase gas-oil-water flows cannot be performed by extrapolating using the this hydrodynamic model. More physics need to be included to account for the effect of the gas phase on the level of turbulence of oil-water liquid mixture, which defines how water droplets will be disrupted and suspended. Moreover, when intermittent flow patterns are present (e.g. slug flow), the impact of the water droplets carried in the liquid mixture

towards the pipe surface can be very violent and develop splashing. This high energy droplet impact can change phase wetting regime of pipe surface in complicated ways.

CONCLUSIONS

- An improved model for predicting full entrainment of water in two-phase oil-water pipe flow has been introduced. It can be directly applied to assess the phase wetting behavior of internal pipe surfaces (oil wet or water wet); and thus, the internal corrosion risk.

- The model consist of a set of hydrodynamic criteria accounting for the estimation of water droplet size and size distribution, the water droplet concentration at the pipe bottom, the hydrodynamic near-wall and boundary layer flow forces to suspend water droplets, and the wettability of internal pipe surfaces.

- The physicochemical influences of the oil-water interface and the oil-water-solid pipe surface interfaces are considered in the present hydrodynamic assessment using the inversion point and the water-in-oil contact angle as inputs.

- The available experimental data on phase wetting transition obtained in a large-scale flow loop for model oil as well as for crude oils show very good agreement with the proposed model.

ACKNOWLEDGEMENTS

The authors want to acknowledge BP, ConocoPhillips, Enbridge, ExxonMobil, Petronas, Shell and Total for their support.

REFERENCES

1. M.B. Kermani, A. Morshed, "Carbon Dioxide Corrosion in Oil and Gas Production - A Compendium," *Corrosion* 59, 8 (2003): p 659.
2. S.N. Smith, M.W. Joosten, "Corrosion of Carbon Steel by H_2S in CO_2 Containing Oilfield Environments," CORROSION/2006, paper no. 6115 (Houston, TX: NACE, 2006), p. 26.
3. U. Lotz, L.v. Bodegom, C. Ouwehand, "The Effect of Type of Oil or Gas Condensate on Carbonic Acid Corrosion," *Corrosion* 47, 8 (1991): p 636.
4. F. Ayello, W. Robbins, S. Richter, S. Nesic, "Model Compound Study of the Mitigative Effect of Crude Oil on Pipeline Corrosion," *Corrosion* 69, 3 (2013): p 286.
5. M. Castillo, H. Rincon, S. Duplat, J. Vera, E. Baron, "Protective Properties of Crude Oils in CO_2 and H_2S Corrosion," CORROSION/2000, paper no. 5 (Houston, TX: NACE, 2000), p. 11.
6. K.D. Efird, J.L. Smith, S.E. Blevins, N.D. Davis, "The Crude Oil Effect on Steel Corrosion - Wettability Preference and Brine Chemistry," CORROSION/2004, paper no. 4366 (Houston, TX: NACE 2004), p. 15.
7. C. Mendez, S. Duplat, S. Hernandez, J. Vera, "On the Mechanism of Corrosion Inhibition by Crude Oils," CORROSION/2001, paper no. 1030 (Houston, TX: NACE 2001), p. 19.
8. S. Richter, M. Babic, X. Tang, W. Robbins, S. Nesic, "Categorization of Crude Oils Based on Their Ability to Inhibit Corrosion and Alter the Steel Wettability," CORROSION/2014, paper no. 4247 (Houston, TX: NACE, 2014), p. 16.
9. J.S. Smart, "Wettability - A Major Factor in Oil and Gas System Corrosion," CORROSION/93, paper no. 70 (Houston, TX: NACE, 1993), p. 15.
10. B.F.M. Pots, J.F. Hollenberg, E.L.J.A. Hendriksen, "What are the Real Influences of Flow on Corrosion?," CORROSION/2006, paper no. 6591 (Houston, TX: NACE, 2006), p. 17.

11. D.T. Tsahalis, "Conditions for the Entrainment of Settled Water in Crude Oil and Product Pipelines," 83rd National Meeting of the AIChE, paper no. (Houston, TX: AIChE[1], 1977), p. 50.
12. M. Wicks, J.P. Fraser, "Entrainment of Water by Flowing Oil," *Materials Performance* 14, 5 (1975): p 9.
13. G.-l. Xu, G.-z. Zhang, G. Liu, A. Ullmann, N. Brauner, "Trapped water displacement from low sections of oil pipelines," *International Journal of Multiphase Flow* 37, 1 (2011): p 1.
14. J.O. Hinze, "Fundamentals of the hydrodynamic mechanism of splitting in dispersion processes," *AIChE Journal* 1, 3 (1955): p 289.
15. S. Arirachakaran, K.D. Oglesby, M.S. Malinowsky, O. Shohan, J.P. Brill, "An Analysis of Oil/Water Flow Phenomena in Horizontal Pipes," SPE Production Operations Symposium, paper no. 18836 (Oklahoma, OK: SPE[2], 1989), p. 13.
16. N. Brauner, A. Ullmann, "Modeling of phase inversion phenomenon in two-phase pipe flows," *International Journal of Multiphase Flow* 28, 7 (2002): p 1177.
17. Y.V.Fairuzov, P. Arenas-Medina, J. Verdejo-Fierro, R. Gonzales-Islas, "Flow Pattern Transitions in Horizontal Pipelines Carrying Oil-Water Mixtures: Full-Scale Experiments," *Journal of Energy Resources Technology* 122, 4 (2000): p 169.
18. ASTM[3] G205 (latest revision), "Standard Guide for Determining Corrosivity of Crude Oils" (West Conshohocken, PA: ASTM).
19. A. Segev, "Mechanistic Model for Estimating Water Dispersion in Crude Oil Flow," Annual AIChE Meeting, paper no. 124a (San Francisco, CA: AIChE, 1984), p. 37.
20. A.J. Karabelas, "Vertical distribution of dilute suspensions in turbulent pipe flow," *AIChE Journal* 23, 4 (1977): p 426.
21. N. Brauner, "The prediction of dispersed flows boundaries in liquid–liquid and gas–liquid systems," *International Journal of Multiphase Flow* 27, 5 (2001): p 885.
22. J.B. Taylor, A.L. Carrano, S.G. Kandlikar, "Characterization of the effect of surface roughness and texture on fluid flow—past, present, and future," *International Journal of Thermal Sciences* 45, 10 (2006): p 962.
23. M. Wegener, N. Paul, M. Kraume, "Fluid dynamics and mass transfer at single droplets in liquid/liquid systems," *International Journal of Heat and Mass Transfer* 71, (2014): p 475.
24. Z.-G. Feng, E.E. Michaelides, "Drag Coefficients of Viscous Spheres at Intermediate and High Reynolds Numbers," *Journal of Fluids Engineering* 123, 4 (2001): p 841.
25. V.Y. Rivkind, G.M. Ryskin, "Flow structure in motion of a spherical drop in a fluid medium at intermediate Reynolds numbers," *Fluid Dyn* 11, 1 (1976): p 5.
26. Institute for Corrosion and Multiphase Technology, Technical Report, "Effect of Water Content on Maximum Droplet Sizes in Oil-Water Dispersed Turbulent Pipe Flow " (Athens, OH: Ohio University, 2015).
27. A.J. Karabelas, "Droplet size spectra generated in turbulent pipe flow of dilute liquid/liquid dispersions," *AIChE Journal* 24, 2 (1978): p 170.
28. P. Angeli, G.F. Hewitt, "Drop size distributions in horizontal oil-water dispersed flows," *Chemical Engineering Science* 55, 16 (2000): p 3133.
29. E.L. Hanzevack, C.B. Bowers, C.-H. Ju, "Study of two-phase flow by laser image processing," *AIChE Journal* 33, 12 (1987): p 2003.
30. R.A. Bagnold, "An Approach to the Sediment Transport Problem From General Physics " (Washington, DC: U.S. Department of the Interior, 1966), p 42.
31. J.L. Trallero, *Oil-Water Flow Patterns in Horizontal Pipes*, PhD thesis (Tulsa, OK: University of Tulsa, 1995).
32. G. El Khoury, P. Schlatter, A. Noorani, P. Fischer, G. Brethouwer, A. Johansson, "Direct Numerical Simulation of Turbulent Pipe Flow at Moderately High Reynolds Numbers," *Flow Turbulence Combust* 91, 3 (2013): p 475.

[1] AIChE, 120 Wall Street, FL 23, New York, NY 10005-4020.
[2] SPE International, 222 Palisades Creek Dr., Richardson, TX 75080.
[3] ASTM International, 100 Barr Harbor Dr., West Conshohocken, PA 19428-2959.

33. J.J. Derksen, R.A. Larsen, "Drag and lift forces on random assemblies of wall-attached spheres in low-Reynolds-number shear flow," *Journal of Fluid Mechanics* 673, (2011): p 548.
34. R.H. Davis, J.A. Schonberg, J.M. Rallison, "The lubrication force between two viscous drops," *Physics of Fluids A: Fluid Dynamics* 1, 1 (1989): p 77.
35. J. Fan, M.C.T. Wilson, N. Kapur, "Displacement of liquid droplets on a surface by a shearing air flow," *Journal of Colloid and Interface Science* 356, 1 (2011): p 286.
36. S. Madani, A. Amirfazli, "Oil drop shedding from solid substrates by a shearing liquid," *Colloids and Surfaces A: Physicochemical and Engineering Aspects* 441 (2014): p 796.
37. B. Mondal, K. Jiao, X. Li, "Three-dimensional simulation of water droplet movement in PEM fuel cell flow channels with hydrophilic surfaces," *International Journal of Energy Research* 35, 13 (2011): p 1200.
38. A.D. Schleizer, R.T. Bonnecaze, "Displacement of a two-dimensional immiscible droplet adhering to a wall in shear and pressure-driven flows," *Journal of Fluid Mechanics* 383, 1 (1999): p 29.
39. X. Zhu, P.C. Sui, N. Djilali, "Three-dimensional numerical simulations of water droplet dynamics in a PEMFC gas channel," *Journal of Power Sources* 181, 1 (2008): p 101.
40. P. Hao, C. Lv, Z. Yao, "Droplet Detachment by Air Flow for Microstructured Superhydrophobic Surfaces," *Langmuir* 29, 17 (2013): p 5160.
41. G.K. Seevaratnam, H. Ding, O. Michel, J.Y.Y. Heng, O.K. Matar, "Laminar flow deformation of a droplet adhering to a wall in a channel," *Chemical Engineering Science* 65, 16 (2010): p 4523.
42. A. Theodorakakos, T. Ous, M. Gavaises, J.M. Nouri, N. Nikolopoulos, H. Yanagihara, "Dynamics of water droplets detached from porous surfaces of relevance to PEM fuel cells," *Journal of Colloid and Interface Science* 300, 2 (2006): p 673.
43. L.G. Sweeney, W.H. Finlay, "Lift and drag forces on a sphere attached to a wall in a Blasius boundary layer," *Journal of Aerosol Science* 38, 1 (2007): p 131.
44. G. Elseth, *An Experimental Study of Oil / Water Flow in Horizontal Pipes*, PhD thesis (Porsgrunn, Norway: The Norwegian University of Science and Technology, 2001).
45. A.M. Mollinger, F.T.M. Nieuwstadt, "Measurement of the lift force on a particle fixed to the wall in the viscous sublayer of a fully developed turbulent boundary layer," *Journal of Fluid Mechanics* 316, (1996): p 285.
46. X. Tang, *Effect of Surface State on Water Wetting and Carbon Dioxide Corrosion in Oil-water Two-phase Flow*, PhD thesis (Athens, OH: Ohio University, 2011).
47. J. Cai, C. Li, X. Tang, F. Ayello, S. Richter, S. Nesic, "Experimental study of water wetting in oil–water two phase flow—Horizontal flow of model oil," *Chemical Engineering Science* 73, 0 (2012): p 334.
48. K.E. Kee, M. Babic, S. Richter, L. Paolinelli, W. Li, S. Nesic, "Flow Patterns and Water Wetting in Gas-Oil-Water Three-phase Flow – A Flow Loop Study," CORROSION/2015, paper no. 6113 (Houston, TX: NACE, 2015), p. 16.
49. K.E. Kee, *A Study of Flow Patterns and Surface Wetting in Gas-Oil-Water Flow*, PhD thesis (Athens, OH: Ohio University, 2014).